

**Water Resources Center  
Annual Technical Report  
FY 2006**

# **Introduction**

**Research Program**

# Use of fluidized bed slag reactors for passive treatment of acid mine drainage

## Basic Information

<b>Title:</b>	Use of fluidized bed slag reactors for passive treatment of acid mine drainage
<b>Project Number:</b>	2006OH32B
<b>Start Date:</b>	3/1/2006
<b>End Date:</b>	6/30/2007
<b>Funding Source:</b>	104B
<b>Congressional District:</b>	6th
<b>Research Category:</b>	Water Quality
<b>Focus Category:</b>	None, None, None
<b>Descriptors:</b>	
<b>Principal Investigators:</b>	Guy Riefler

**Publication**

# USE OF FLUIDIZED BED SLAG REACTORS FOR PASSIVE TREATMENT OF ACID MINE DRAINAGE

## *One Year Progress Report*

Guy Riefler  
Department of Civil Engineering  
Ohio University  
Athens, Ohio 45701

### **Problem and Research Statement**

Coal production has been a major industry in Ohio and because of increasing pressure on petroleum reserves will likely continue into the future. Mining however can have a significant negative impact on water resources, and abandoned underground mines continue to be a serious threat to water quality in southeast Ohio. Ohio coal deposits contain significant quantities of pyrite. As water and oxygen are supplied to these underground pyrite reserves by abandoned mine shafts, chemical and biological reactions oxidize the pyrite forming high concentrations of sulfuric acid and dissolved iron. The resulting low pH also dissolves other metals, typically aluminum being of greatest concern in Ohio. Water released from these mine shafts carry very high acid and metal loads that can kill aquatic life in a stream for miles downstream. For the past twenty years, southeast Ohio has devoted millions of dollars to reducing the impact of this acid mine drainage (AMD). Yet AMD remains a leading cause of surface water pollution in southeast Ohio.

One particularly difficult type of AMD source to treat occurs when a large mine complex empties near an impact point with no space for installation of a large passive treatment system. Active treatment systems are sometimes employed such as alkaline dosing, but the ongoing maintenance costs pose a problem for managing agencies. In the past five years, waste iron slag has emerged as an attractive treatment alternative. When iron ore is melted and purified, slag is the waste product that floats to the top of the melt and is discarded. It is strongly alkaline and inexpensive. When used for AMD treatment, the acidic water is directed through lined pits filled with uniformly sized pieces of slag. However, the elevated pH results in precipitation of metals, primarily iron and aluminum. The metals may clog and armor the slag which over time leads to hydraulic clogging of the slag bed and reductions in alkalinity addition. As a result, slag beds are often used only when a clean water source can be found. Thus, clean water flows through the slag bed, raising the pH to approximately 11 which is then mixed with the AMD. This is a very effective, inexpensive, and treatment option, although, it is only possible at sites with a clean water source, room for installation of the bed, and room for installation of a wetland to collect the metals precipitates before reaching the impact point.

This research tested the effectiveness of a novel treatment configuration. Fluidized bed reactors are extremely efficient, providing significant surface contact time in a very small footprint. Engineered systems like these are seldom considered for AMD treatment because of the energy requirements to fluidize the bed. However, abandoned mine flows often have sufficient pressure to provide enough head for fluidization of the bed. Further, the agitation of the slag particles will allow metal precipitates to flow out of the bed preventing clogging. It is likely that scouring of the slag particles will also prevent armoring and maintain continuous alkalinity addition, until the particles require replacement. In short, this research tests a new treatment technology that if successful will have application to some of our most troublesome AMD sources.

## Methodology

The first portion of this experiment was to determine the rate at which different sieved slag fractions fluidized using a fluidized bed reactor. The reactor was composed of a large glass chromatography column 4" inner diameter and 24" length (ACE Glass Incorporated, Vineland, NJ; see Figure 1). Slag fines were supported by a plastic frit supplied with the column. Water flowed through a Materflex adjustable peristaltic pump and a flow equalizer to eliminate pulsing before entering the bottom of the column. pH into and out of the fluidized bed was measured using a WTW Multi 350i pH meter and a Denver Instrument Model 225 pH meter. Influent and effluent samples were periodically collected and analyzed for acidity and alkalinity using standard methods (Standard Methods, 20th Edition, 1998).

Slag sand was obtained from Tube City IMS (Horsham, PA), a company that specializes in slag recovery. Chemical analysis from the company indicated a pH of 12.6 and calcium carbonate equivalent of 612,000 mg/kg for the slag. Slag fines were sieved using #20, #40, and #60 sieves and the fractions were saved. These sieves have mesh sizes of 850  $\mu\text{m}$ , 425  $\mu\text{m}$ , and 250  $\mu\text{m}$  respectively. Mine spoil or gob was collected from a local site that was known to produce significant AMD. A 20-gallon tub was filled with gob and flooded with tap water. After several days, pH and acidity in the water was 2.8 and 170 mg  $\text{CaCO}_3/\text{L}$ .

Three tests were performed with this fluidized bed reactor. First, the three different slag sizes were tested at different flow rates to determine flow required for fluidization. Next, effluent pH with clean water running through the fluidized bed was determined. Finally, AMD generated from the gob pile was delivered through the fluidized bed, and effluent pH and alkalinity and acidity concentrations measured.

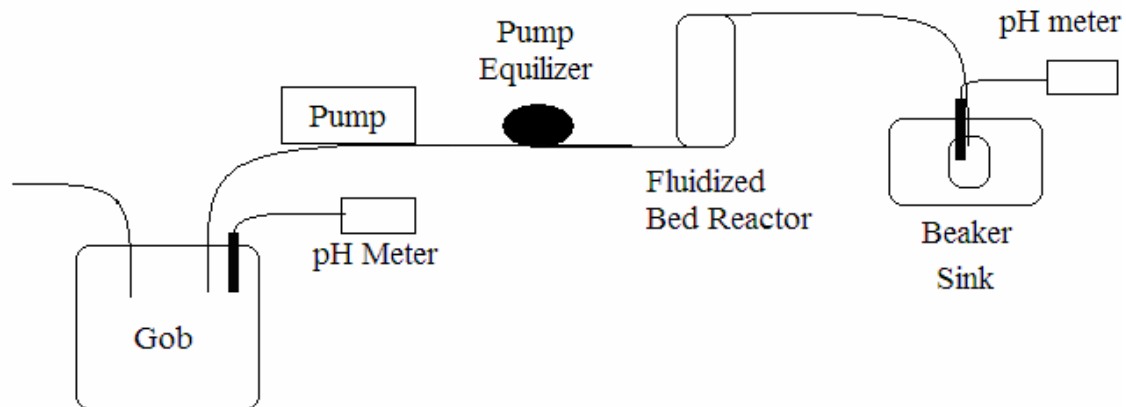


**Figure 1: Fluidized Bed Reactor Setup**

## Principal Findings

### *Fluidization of Slag*

The first part of this project was to determine the flow rate at which different sizes of slag particles fluidize. Originally a glass frit was used, but the glass frit did not allow the fluid to flow at a sufficient rate. It was determined that the plastic frit that was provided with the original glassware produced better results. Below are the tables showing the fluidization tests with the plastic frit of slag particles from #20, #40, and #60 sieves.

Flow Rate (mL/min)	Description for 1" #20 slag layer	Flow Rate (mL/min)	Description for 1.25" #20 slag layer
100	No movement	100	No movement
200	No movement	200	No movement
300	No movement	300	There was some small shaking in a vibrating like motion.
400	No movement	400	There was some small shaking in a vibrating like motion.
500	There was some small shaking in a vibrating like motion.	500	There was some small shaking in a vibrating like motion.
600	There was little movement of small particles on top layer.	600	There was some small shaking in a vibrating like motion.
700	There was little movement of small particles on top layer.	700	There was some small shaking in a vibrating like motion.
800	There was little movement of small particles on top layer.	800	There was faster shaking in a vibrating like motion.
900	One tunnel of movement 3/4in wide.	900	There was some small movement of slag pieces in one 1in section.
1000	Single tunnel flowing faster	1000	There was faster movement of slag pieces in one 1in section.
1100	Single tunnel was about 1in wide and flowing faster. Little to no movement in other areas.	1100	Faster movement in 1.25in section. Little to no movement in other areas.

1200	Single tunnel was now about 1in wide and flowing faster. Little to no movement in other areas.	1200	Faster movement in 1.5in section. Little to no movement in other areas. Section in motion raised 1/16in.
1300	Single tunnel is now about 1 in wide and flowing faster. Little to no movement in other areas.	1300	Faster movement in 1.5in section. Little to no movement in other areas. Section in motion raised 1/16in.
1400	Another section was starting to flow about 1.25in wide. Section in motion was raised 1/4in.	1400	Section in motion was raised 1/8in. 1 in of moving perimeter was fluidized.
1500	1/4 of perimeter was fluidized. Little to no movement in other areas.	1500	1.75in of perimeter was in motion. 1.25in fluidized. Little to no movement still in other areas.
1600	1/4 of perimeter was fluidized. Little to no movement in other areas. Tunnel was raised 1/4in.	1600	1.5in fluidized. Section in motion was raised 1/4in.
1700	1/4 of perimeter is fluidized. Little to no movement in other areas. Tunnel was raised a little under 1/2in.	1700	2in of perimeter was in motion. 1.5in fluidized.
1800	About 1.75in of perimeter was fluidized.	1800	1.75in fluidized. Section was in motion raised 5/16in.
1900	2in of perimeter was fluidized.	1900	Faster movement
2000	Section in motion raised 5/8in and flowed faster.	2000	Faster movement
2100	Section in motion was raised 3/4in and flowing faster.	2100	2in of perimeter was fluidized. There was little to no movement in other areas.
>2100	Fluidized section grew a little in height and the speed of flow increased with increasing flow rate. Areas not fluidized had little to no movement.	2200	Fluidized section raised 3/8in.
		2300	2.125in fluidized. Fluidized section raised just under 1/2in.
		2400	Faster motion
		2500	2.125in fluidized. Fluidized section raised just under .5in.
		2600	Fluidized section grew a little in height and the speed of flow increased with increasing flow rate. Areas not fluidized had little to no movement.

**Table 1: Fluidization results at different flow rates using #20 slag**

Table 1 shows that #20 slag started to have sections fluidize around 1500 mL/min. In trial 1 the maximum amount fluidized was 2 in of the perimeter, this occurred at 1900 mL/min. In trial 2 the maximum amount fluidized was 2.125 in of the perimeter and this happened at 2300 mL/min. Significant fluidization was not achieved with this size slag at any flow rate.

<b>Flow Rate (mL/min)</b>	<b>Description for 1.25" #40 slag layer</b>	<b>Flow Rate (mL/min)</b>	<b>Description for 1.5" #40 slag layer</b>
100	No movement	100	No Movement
200	One small tunnel formed with very slow movement. The slag as a whole was in a wave like vibration.	200	There was some shaking of whole mass
300	Same wavelike vibration, but faster	300	There was some shaking of whole mass
400	Original tunnel grew and was 3/4in wide. Small tunnels formed in bottom half of slag.	400	Faster shaking. There was some movement of particles in 1/4 of perimeter.
500	Original tunnels became wider. Other tunnels formed with slower flow.	500	Faster shaking. There was some movement of particles in 1/4 of perimeter.
600	1/2 of perimeter was in motion. The slag has raised 1/16in.	600	More tunnels were formed toward the top. Slag was raised 1/16in. 1/4 of perimeter had motion
700	Faster motion in perimeter. Instead of tunnels the slag was moving in sections. 2/3 of perimeter had movement	700	1/4 fluidized. There was some movement in 1/2 of perimeter.
800	1/3 of perimeter fluidized. Faster flow in other formed tunnels.	800	There was faster movement in 1/2 of perimeter. Slag has raised 1/8in
900	1/2 of perimeter was fluidized. Slag has raised 1/4in	900	1/3 of perimeter was fluidized. Faster movement in another 1/3 of perimeter. Slag had raised 3/16in.
1000	1/2 of perimeter was fluidized. Slag was raised 1/4in. There was faster movement of slag.	1000	1/3 of perimeter was fluidized. There was faster movement in another 1/3 of perimeter. Slag had raised 1/4in.
1100	2/3 of perimeter fluidized. There was faster movement of slag.	1100	1/2 of perimeter was fluidized. Slag had raised 7/8 in

1200	2/3 of perimeter was fluidized. There was faster movement of slag.	1200	2/3 of perimeter fluidized. Other areas had little to no movement.
1300	There was faster higher flow in fluidized areas.	1300	There was faster movement in fluidized areas.
1400	1/3 of slag had little to no movement. There was fast fluidization in all other areas.	>1300	Movement in fluidized areas just sped up with increasing flow rates. Areas with little to no movement remained that way.
1500	1/3 of slag had little to no movement. Fast fluidization in all other areas.		
>1500	Above 1500 flow of areas already fluidized just increases and the areas with little to no movement did not change.		

**Table 2: Fluidization results at different flow rates using #40 slag**

Table 2 shows that Sieve #40 started to fluidize around 800 mL/min. In both trials it shows that 2/3 of the perimeter fluidized was the maximum amount of area fluidized. This occurred around 1200 mL/min in both trials.

Flow Rate (mL/min)	Description for 1" #60 slag layer
100	Two sections showing shaking motion
200	As a whole slag raised 1/16in. 2in wide was in motion on one side. 1.5 in wide on other side. As a whole showed shaking flow.
300	1/2 of perimeter showed faster shaking motion. Slag as whole raised 1/8in. 2.25in wide tunnels raised.
400	Section in motion flowed faster. Slag as a whole raised .25in. .25in of perimeter was fluidized
500	1in of perimeter fluidized. Other areas moving faster. Other sections little to no movement.
600	About 2in of perimeter fluidized. Slag raised .5in.
700	1/2 of perimeter fluidized. Tunnels forming in sections that previously had no movement.
800	80% of perimeter is fluidized. No movement in 10% of slag.
900	85% fluidized. 10% has little to no movement.
1000	90% fluidized. 10% has little to no movement.
1100	90% fluidized. 10% has little to no movement.
>1100	There were no extreme differences in the movement of the slag after 1100 and fluidization was never reached at the speeds produced.

**Table 3: Fluidization results at different flow rates using #60 slag**

Table 3 shows that fluidization occurred at an even lower flow rate with the #60 slag, with the bed expanding with flow rates as low as 400 mL/min and near complete fluidization at 800 mL/min. Even at higher flow rates, however, approximately 10% of the bed never fluidized.

The previous set of experiments showed varying degrees of fluidization with different slag grain size and flow rates. Often partial fluidization would occur, that is, only a small portion of the slag layer would show significant movement, while the remainder of the layer stayed fixed. Consequently there was not a clear demarcation for the beginning of fluidization. Further even at high flow rates, a portion of the bed always remained fixed.

These results indicate that #20 slag was too large to adequately fluidize at flow rates less than 2500 mL/min and would not be suitable for the apparatus in this experiment. We chose #40 slag at a flow rate of 800 mL/min which provided adequate movement of the particles at a flow rate that our experimental set-up could accommodate. For scaling up of the reactor to a field site, however, these results were discouraging. It required significant flow to fluidize only a 1 in thick layer of fine particle slag. The high flow rate reduces the retention time in the reactor and limits the ability of the slag to release alkalinity. Clearly a deeper layer of slag will be required; however it seems not possible to fluidize it. Also, the fine particles will likely be exhausted of alkalinity earlier than the larger slag particles.

### ***Fluidized Bed Treatment of AMD***

The first test that was conducted was running the fluidized bed reactor system with tap water and the Sieve #40 slag at a flow rate of 800 mL/min. For this test only the pH exiting the system was recorded every 20 seconds for 3000 seconds, and pH results are shown in Figure 2. Influent pH to the reactor remained near 7.2 for the duration of the experiment. Initially, pH increased over 9 but then decreased to a fairly stable value of 8.1. The initial high pH was likely due to rapidly dissolving slag fines that were quickly exhausted. The stable exit pH of 8.1 was not significantly higher than the inflow. This was likely due to the short retention time as the water flowed through the one inch layer of slag.

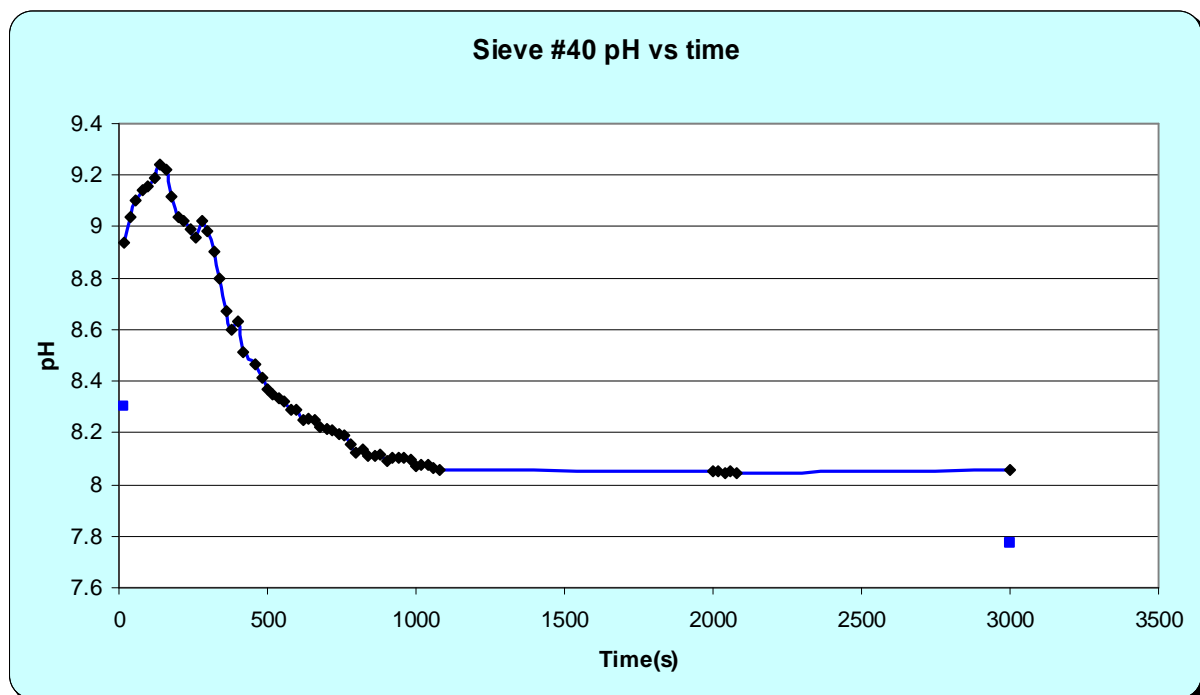


**Figure 2: Effluent pH with a 1-inch layer of # 40 slag, a flow rate of 800mL/min, and tap water.**

For the next test, AMD generated by the submerged gob was used as influent to the fluidized bed reactor. In order to increase retention time, a 2 in layer of #60 slag was used at a flow rate of 800 mL/min. pH measurements were taken at the entrance and exit every minute for one hour. Samples were taken at 0, 5, 20, 40 and 60 minutes and analyzed for alkalinity and acidity. pH results are shown in Figure 3, and acidity and alkalinity results are shown in Figure 4.

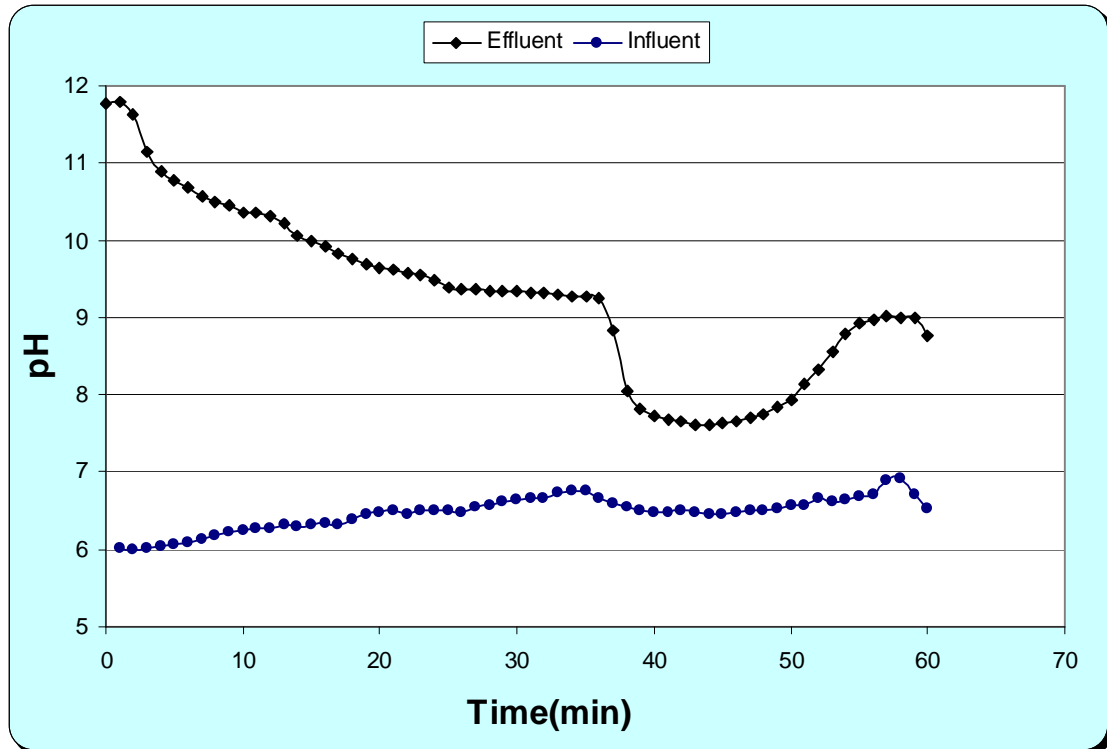


**Figure 3: Influent and effluent pH with slag #60, a bed depth of 2 in, a flow rate of 800 mL/min, and acidic influent.**

In this test, very high pH values were obtained in the effluent of the fluidized bed reactor, even with acidic input. Effluent pH started at near 12 but decreased gradually to a value of 7.6 after approximately 40 minutes. It did recover somewhat for unknown reasons reaching a pH of 9. The alkalinity and acidity results showed more consistent results. Initially 220 mg CaCO<sub>3</sub>/L was generated which decreased rapidly to between 100 and 150 mg CaCO<sub>3</sub>/L. Acidity was zero initially, before acidic water from the gob had reached the effluent. Acidity continually increased reaching a value of 143 mg CaCO<sub>3</sub>/L by the end of the test, however it may have continued to climb beyond the test to close to the influent acidity of 170 mg CaCO<sub>3</sub>/L. This residual acidity was likely in the form of hydrolysable metals that were not detected in the alkalinity test. Indeed during the hot peroxide pretreatment for the acidity test, the samples turned orange due to the oxidation and hydrolysis of ferrous iron. According to standard analytical methods the hot peroxide pretreatment step is only performed on the acidity test, not the alkalinity test, thus resulting in the seemingly contradictory result that a sample can have both positive acidity and alkalinity.

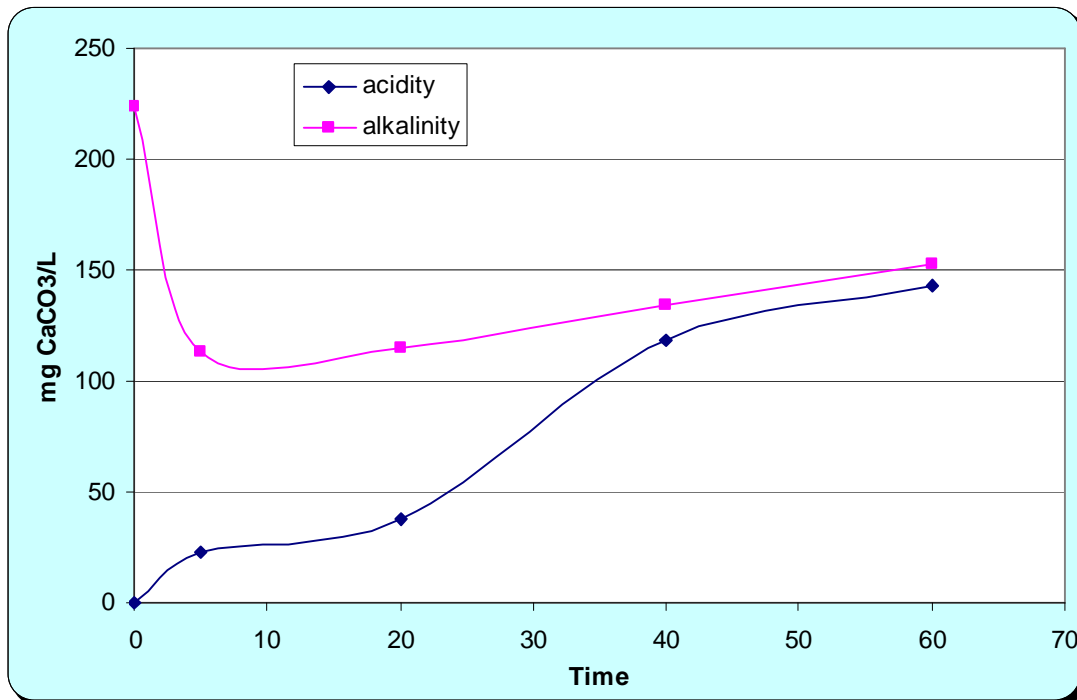


**Figure 4: Effluent alkalinity and acidity plotted against the time with slag #60, a bed depth of 2 in, a flow rate of 800 mL/min, and an acidic influent.**

## Significance

These results indicate that this treatment approach has significant limitations both with regard to hydraulics and chemical transport. First, the slag particles proved difficult to fluidize requiring the use of very small grain size. #20 slag was too large to adequately fluidize, although #40 slag and #60 slag could be adequately fluidized with bed depths of 1-2 inches. For scaling up of the reactor to a field site, these results were discouraging. These particles are extremely fine and would likely increase costs significantly to crush and sieve the slag material to this size window for full-scale implementation. Further, it required significant flow to fluidize only a 1 in thick layer of fine particle slag. The high flow rate reduces the retention time in the reactor and limits the ability of the slag to release alkalinity. Clearly a deeper layer of slag will be required; however it seems not possible to fluidize it. Also, the fine particles will likely be exhausted of alkalinity earlier than the larger slag particles.

The water chemistry results were a little more encouraging. With a 1 inch layer of #40 slag, pH of tap water was increased only to around 8.1 from 7.2, not a very significant improvement. Further experiments were conducted with 2 inch layers of #60 slag. When treating lab generated AMD, pH was held to about 8 again but initially reaching pH as high as 12. Further there was consistent delivery of alkalinity between 100 and 150 mg CaCO<sub>3</sub>/L. Unfortunately only a portion of the acidity was neutralized and that continued to decrease over the course of the experiment. From these experiments, it appears this small a slag layer is not able to treat AMD

significantly, and deeper slag layers face hydraulic limitations preventing fluidization. Continued research is being conducted to investigate these issues further.

# Characterizing and Controlling Membrane Biofouling

## Basic Information

<b>Title:</b>	Characterizing and Controlling Membrane Biofouling
<b>Project Number:</b>	2006OH34B
<b>Start Date:</b>	3/1/2006
<b>End Date:</b>	2/28/2007
<b>Funding Source:</b>	104B
<b>Congressional District:</b>	1
<b>Research Category:</b>	Engineering
<b>Focus Category:</b>	Water Quality, Water Supply, Treatment
<b>Descriptors:</b>	None
<b>Principal Investigators:</b>	Daniel Barton Oerther, Dionysios Dionysiou

## Publication

1. Zhang, K., Choi, H., Dionysiou, D., Sorial, G., and Oerther, D.B., 2006, Identifying Pioneer Bacterial Species Responsible for Biofouling Membrane Bioreactors, *Environmental Microbiology, Society for Applied Microbiology and Blackwell Publishing*, 8(3):433-440
2. Oerther, D.B., 2006, Integrating Molecular Biology Research, Teaching, and Professional Outreach in Environmental Engineering and Science, *Journal Environmental Engineering Science, Mary Ann Liebert, Inc.*, 23(3):451-460
3. Choi, H., Zhang, K., Dionysiou, D.D., Oerther, D.B., and Sorial, G.A., 2006, Membrane filtration performance with activated sludge of CSTR and PFR for the treatment of paper mill wastewater, *Chemosphere, Elsevier*, 63(10):1699-1708
4. Lu, T., Saikaly, P.E., and Oerther, D.B., 2007, Modeling Competition of Aerobic Heterotrophs for Complementary Nutrient in a Biofilm Reactor: Effect of Hydraulic Retention Time on Coexistence, *Water Science and Technology, International Water Association*, 55(8-9):227-235
5. Zhang, K., Choi, H., Wu, M., Sorial, G.A., Dionysiou, D., and Oerther, D.B., 2007, An Ecology-based Analysis of Irreversible Membrane Biofouling in MBRs, *Water Science and Technology, International Water Association*, 55(8-9):395-402
6. Wu, M.Y., Suryanarayanan, K., van Ooij, W.J., and Oerther, D.B., 2007, Using Microbial Genomics to Evaluate the Effectiveness of Silver to Prevent Biofilm Formation, *Water Science and Technology, International Water Association*, 55(8-9):413-419

**Grant title:** Characterizing and Controlling Membrane Biofouling  
**PI:** Daniel B. Oerther, Ph.D., PE, BCEE, Department of Civil and Environmental Engineering, University of Cincinnati, Box 210071, Cincinnati, OH 45221-0071; [Daniel.Oerther@uc.edu](mailto:Daniel.Oerther@uc.edu); 513-556-3670, voice; 513-556-2599, fax  
**Co-PI:** Dionysios D. Dionysiou, Ph.D., Department of Civil and Environmental Engineering, University of Cincinnati, Box 210071, Cincinnati, OH 45221-0071; [Dionysios.Dionysiou@uc.edu](mailto:Dionysios.Dionysiou@uc.edu); 513-556-0724, voice; 513-556-2599, fax  
**Start date:** March 1, 2006  
**End date:** February 28, 2007  
**Total project:** \$92,450  
**USGS:** \$28,127

**Problem and Research Objective.** The application of membranes to separate particulate and suspended materials from water streams is an evolving technology. Membrane unit operations have many advantages as compared to conventional treatment technology that rely upon clarifiers and filtration to remove suspended materials. The primary disadvantages of membrane unit operations include capital costs for the membranes and operating costs associated with routine membrane cleaning. Biofouling is a serious problem for the operation of membrane unit operations because it results in decreased transmembrane fluxes. For this project, we hypothesize that preventing the initiation of biofilm formation on membrane surfaces is the best approach for eliminating biofouling. To scientifically test this hypothesis, we investigated the fundamental mechanisms of biofilm initiation on membrane surfaces.

The overall objective of this collaboration is to identify approaches to eliminate fouling of membrane surfaces due to the action of biological components. To accomplish this objective, our research team examined the initiation of biofilm formation on membrane surfaces through a synergistic study of the physicochemical properties of select membranes; the impact of various water streams on the physicochemical properties of select membranes; the biochemical interactions between microorganisms and select membranes; and the role of microbial ecology in the initiation of biofilm formation on membrane surfaces.

Four Tasks were undertaken:

**TASK ONE** existing laboratory-scale membrane unit operations were challenged with water (e.g., distribution system pipe loop) and wastewater (e.g., mixed liquor from activated sludge and/or membrane bioreactor systems) samples as well as mock environmental samples (e.g., clean water dosed with pure cultures of specific microorganisms or commercially available humic acids);

**TASK TWO** biofouling of membranes was quantified using an improved version of an existing conceptual and mathematical model relating transmembrane flux to fouling;

**TASK THREE** selective accumulation of microorganisms on membrane surfaces was documented using available genome-enabled molecular biotechnologies; and

**TASK FOUR** broad dissemination will be achieved through organizing and conducting a preconference workshop at State of Ohio Water Environment Association meeting with a focus on characterizing and preventing membrane biofouling.

**Methodology.**

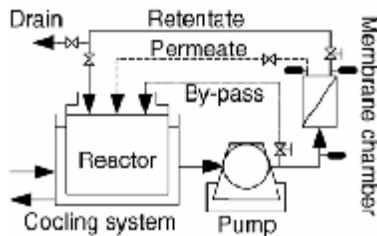


Fig 1. Schematic of lab-scale membrane system.

With prior USGS funding, we designed, constructed, and operated a laboratory-scale membrane reactor system shown in Figure 1. Flat sheets (72 square centimeters) of Osmonics PVDF microfiltration (0.3 micron nominal pore size) or ultrafiltration (30,000 Dalton molecular weight cut off) membrane were operated at 20°C with a transmembrane pressure of 100 kPa and constant cross flow velocities of 0.3, 1, 2, 3.5, or 4.5 m/sec. During the period of operation, transmembrane flux was measured

continuously. Reduced transmembrane flux observed over time was presumed to be linked to membrane fouling using a resistance in series model. To complete Task One, the existing membrane system were challenged with water samples collected from existing full-scale and laboratory-scale bioreactors (e.g., Mill Creek wastewater treatment plant located at 1600 Gest St, Cincinnati, Ohio) as well as samples of water collected from full-scale municipal drinking water production plants on the Ohio River (e.g., Miller Treatment plant in California, Ohio and the US EPA Test and Evaluation Facility located at 1600 Gest St, Cincinnati, Ohio). These water samples were placed in the reactor tank and maintained at a constant temperature. Each water sample was characterized according to Standard Methods for the Examination of Water and Wastewater (including determinations of Total Solids, Suspended Solids, Volatile Solids, Volatile Suspended Solids, Total Particle Counts, and Cell Abundance by staining). Vacuum filtration was performed with samples of representative membranes listed in Table 2. Optimal filtration times (defined as steady-state permeate flux) were determined experimentally and were approximately 5 hours (with a flow rate of 20 liters/square meter of membrane/hr).

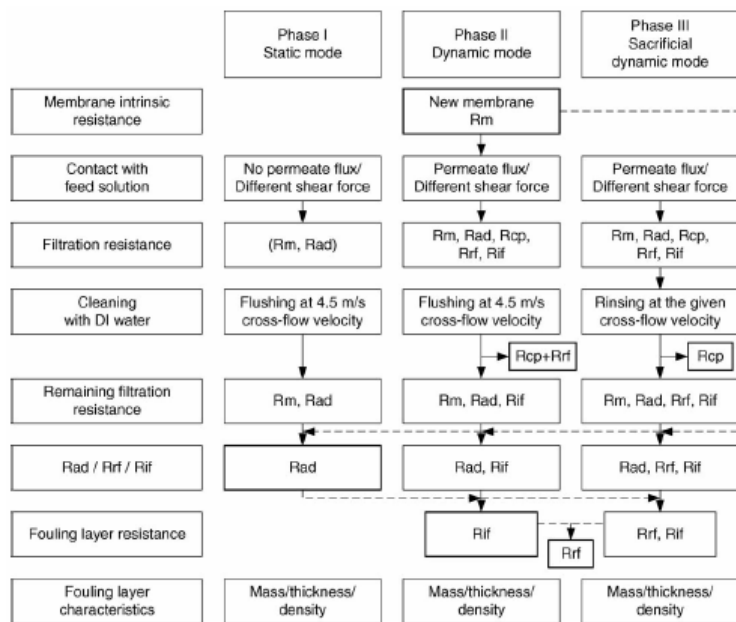
The membranes tested in this study are presented in Table 1.

Table 1. Membranes proposed to be tested in Task One.

Company	Materials	Interaction with H <sub>2</sub> O	Pore size or MWCO
Osmonics	Nitrocellulose	Hydrophilic	0.1 μm
	Cellulose acetate	Hydrophilic	0.22 μm, 20K
	Polycarbonate	Slightly hydrophobic	0.1, 0.2 μm
	Polypropylene	Hydrophobic	0.1, 0.22 μm
	Polysulfone	Hydrophobic	30K, 60K
	Polyamide	Hydrophobic	4K
	Polyethersulfone	Hydrophobic	5K, 20K
	Polyvinylidene fluoride	Hydrophobic	0.3 μm, 30K
Mitsubishi Rayon <sup>1</sup>	Polyethylene	Hydrophobic	0.1 μm

In addition to testing environmental samples, we used standard aseptic techniques to prepare pure cultures of representative microorganisms including *Escherichia* and *Acinetobacter*. Batches of pure cultures were prepared on standard media, and diluted to

a concentration of less than 1,000 mg volatile suspended solids per liter (e.g., wastewater) to one million colony forming units per one hundred milliliters (e.g., surface water) using phosphate buffered saline. Filtration tests were performed with these pure cultures using the same standard operating procedure followed for the environmental samples. To test the impacts of EPS on irreversible biofouling, we dosed synthetic EPS compounds into the membrane flow cell. Nucleic acid (reagent grade DNA), polysaccharide (reagent grade alginate), and protein (reagent grade casein) were examined.



Membrane biofouling was characterized using a well-described resistance in series model coupled with the characterization protocol presented in Figure 2. Biofouling was defined as irreversible resistance (that cannot be removed by flushing with a cross flow velocity of 4.5 m/sec). Irreversible resistance was calculated as the resistance after flushing minus the intrinsic resistance minus the resistance due to adsorption.

Fig. 2. Flow chart outlining the procedure for membrane characterization to determine intrinsic ( $R_m$ ), reversible ( $R_{r,f}$ ), and irreversible ( $R_{i,f}$ ) membrane fouling based upon adsorption ( $R_{ad}$ ), concentration polarization ( $R_{cp}$ ), resistance after flushing ( $R_{r,f}$ ), and resistance after rinsing ( $R_{r,r}$ ).

In prior work, we used 16S ribosomal DNA targeted molecular biology tools to fingerprint microbial communities irreversibly bound to membrane surfaces, and we compared these fingerprints with the identity of the microbial populations present in suspension. As shown in Figure 3, for Osmonics PVDF microfiltration membrane, biofouling of the membrane surface was due to the irreversible adhesion of specific microbial populations (e.g., *Asticcacaulis* spp.) that were not present in abundance in suspended form (e.g., predominance of *Zoogloea* spp. in suspension). This result was unanticipated as prior engineering assumptions indicated that all microorganisms were equally likely to cause irreversible biofouling. For this project we used existing 16S rDNA-targeted techniques available in our laboratory including Amplified Ribosomal DNA Restriction Analysis (ARDRA) as well as cloning and sequencing.

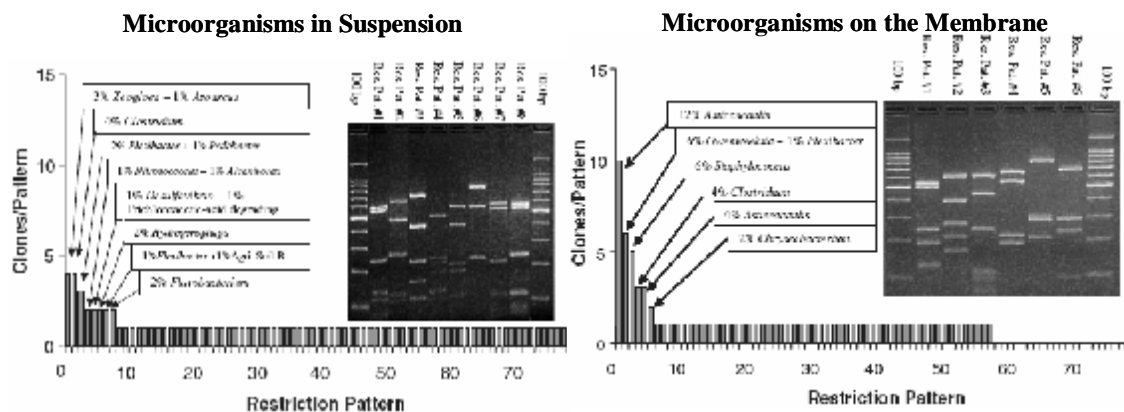


Fig. 3. Composition of the microbial communities in suspension and irreversibly attached to membrane surfaces during vacuum filtration with Osmonics PVDF microfiltration membrane.

Briefly, genomic DNA was extracted using commercial Soil DNA Extraction kits (MoBio, Inc.) following the manufacturer's instructions. Polymerase chain reaction (PCR) targeting 16S rDNA will be performed using primers S-D-Bact-0011-a-S-17 (5' GTTTGATCCTGGCTCAG) and S-D-Bact-1492-a-A-21 (5' ACGGYTACCTTGTACGACTT) with Takara Ex Taq. PCR products were verified using 1% agarose gel electrophoresis. Cloning will be performed using the Topo TA Cloning Kit (Invitrogen, Inc.) according to the manufacturer's instructions. Plasmid inserts were amplified by PCR using primers M13 (-21) (5' TGAAAACGACGGCCAGT) and M13 Reverse (5' CAGGAAACAGCTATGAC). Restriction digests for ARDRA were performed using the endonuclease MspI according to the manufacturer's instructions (Promga). ARDRA were performed using agarose gel electrophoresis and an available Kodak digital gel documentation system. For sequencing, individual clones were subcultured and plasmid DNA was extracted using QIAprep Spin Miniprep Kit (QiaGen) according to the manufacturer's instructions. Semi-automated DNA sequencing was performed on a fee-basis by the DNA Core Laboratory of the University of Cincinnati using primer S-D-Bact-0338-a-S-18 (5' ACTCCTACGGGAGGCAGC). Sequencing results were analyzed using BLAST as well as an available Linux workstation running ARB. These experiments were used to identify the predominant microbial populations present on the membrane surface as well as in suspension. By comparing the composition of these two microbial communities, we identified which membrane surfaces provide selective environments to accumulate specific microbial populations.

All experiments were performed using existing laboratory-facilities available at the University of Cincinnati.

### Principal Findings and Significance.

In previous work, an experimental procedure and model were developed to estimate irreversible biofouling from laboratory-scale membrane component testing data. This model and experimental procedure was extended to examine biofouling of biomass from a variety of sources including: activated sludge biomass from full-scale municipal sewage treatment plants; natural biomass from surface waterways; biomass from laboratory-scale

membrane bioreactor sewage treatment plants; and pure cultures of select microorganisms. The biomass was further characterized by a number of experimental parameters including: composition of extracellular polymeric substances (EPS); floc size; and zeta potential. In addition, genome-enabled molecular biology-based techniques were used to identify and quantify predominant bacterial populations present in the mixed liquor suspended growth biomass as well as in adhered sessile biofilms.

The major findings included the following observations:

- The identity of members of microbial communities irreversibly bound to membrane surfaces can be very different from the identity of membranes of microbial communities found in suspended growth bioreactors.
- Members of the Alpha-subclass of the Proteobacteria including *Brevundimonas* and *Asticcacaulis* are more likely to irreversibly bind to membranes.
- Members of the Gamma-subclass of the Proteobacteria including *Acinetobacter* are more likely to irreversibly bind to membranes.
- Some members of the Low G+C content of the Gram Positive Bacteria including *Staphylococcus* spp. are more likely to irreversibly bind to membranes.
- Students and adult practitioners of environmental engineering can be introduced to the benefits of genome-enabled molecular biology-based techniques for identifying and quantifying microbial populations in environmental samples through one-day long workshops and seminars which include hands-on activities accompanying lecture-discussion formats for information dissemination.
- Bioreactor operation in a plug-flow mode resulted in a microbial community which was less likely to produce irreversible biofouling as compared to a microbial community developed in a bioreactor operated in a completely-mixed mode.
- *Acinetobacter calcoaceticus* and *Gordonia amarae* are more likely to result in irreversible biofouling as compared to a similar abundance of *Escherichia coli* suggesting that specific bacterial populations may be more prone to the initiation of irreversible biofouling.
- Mathematical modeling of the competition of six theoretical bacterial populations competing for three growth limiting nutrients in a steady-state biofilm of constant thickness with variable density showed that different biofilm conditions favored different amounts of diversity in the bacterial community.
- Bioreactor operating conditions which influenced the diversity of the bacterial community were different for three base cases including: fully penetrated; internal mass transfer resistance; and external mass transfer resistance.

In summary, the results of this project suggest that specific bacterial populations are responsible for the initiation of biofouling in membrane bioreactors. Furthermore, operating conditions selected by engineers in the design of membrane bioreactors could influence microbial community composition and its physical properties. Thus, the ability to reduce biofouling in membrane bioreactors can be influenced by the operating conditions selected by the engineers during the system design phase.

Future work should examine if engineering design decisions can influence biofouling in long term studies through selective control of microbial community composition. Furthermore, studies of molecular microbial ecology should be conducted to specifically elucidate the mechanism whereby this potential level of control can be used.

# Development of a Novel Hydrogel-Based Sensor for the Detection of Biological Contaminants

## Basic Information

<b>Title:</b>	Development of a Novel Hydrogel-Based Sensor for the Detection of Biological Contaminants
<b>Project Number:</b>	2006OH35B
<b>Start Date:</b>	3/1/2006
<b>End Date:</b>	2/28/2007
<b>Funding Source:</b>	104B
<b>Congressional District:</b>	9th District: Lucas County, OH
<b>Research Category:</b>	Water Quality
<b>Focus Category:</b>	Surface Water, Water Quality, Non Point Pollution
<b>Descriptors:</b>	
<b>Principal Investigators:</b>	Cyndee Gruden

## **Publication**

1. Gruden, C.L., Escobar, I., Coleman, M., Gorey, C., and Mileyeva-Biebesheimer, O. 2007. Polymer brush based bacterial sensors for improved membrane performance in 33rd Regional Meeting of ACS. Covington, KY.
2. Gruden, C.L., Escobar, I., Coleman, M., Gorey, C., and Mileyeva-Biebesheimer, O. 2007. Development of fouling resistant water treatment membranes with microbial sensing capabilities in 34th National Meeting of ACS, Boston, MA.
3. Escobar, E., Gruden, C., and Coleman, M. 2007. Development of fouling resistant water treatment membranes with microbial sensing capabilities Controlled Environments Magazine. In Press.

**PROJECT TITLE.** Development of a Novel Hydrogel-Based Sensor for the Detection of Biological Contaminants

**PROJECT TEAM.** Cyndee L. Gruden, Olya Mileyeva-Biebesheimer (PhD student), Sun Gi Kim (PhD student), Natalie Bailey (BS student)

Department of Civil Engineering, University of Toledo, Toledo, OH.

**PROBLEM.** Coastal water quality is an important issue from a public health and an economic standpoint. A variety of diseases, including gastroenteritis, dysentery, and hepatitis, can be carried to coastal areas via contaminated waters. In addition, surface waters in the Great Lakes Region also act as source waters for surrounding communities. There is a keen interest in tracking and eliminating potential pathogens in these systems. Admittedly, much attention has been given to sensor development in the past several years, however, sensors that exhibit strong and selective binding for biological targets are still needed. Most rapid detection assays are affinity-based, where organism-specific biomolecules, such as artifacts (e.g., exocellular proteins, fatty acid composition) or genomic material (e.g., DNA, rRNA) are targeted. Once the target biomolecule is identified, the sensor must have the specificity to identify a target biomolecule in a complex system and the sensitivity to detect its presence, even at low concentration. Immunochemical assays, which rely on antibody (Ab) affinity to target analytes, are arguably the most frequently used biosensors due to their simplicity, rapid response, and financial viability (Ivnitski et al., 1999; Iqbal et al., 2000). For specific detection, antibodies (Ab) can be immobilized on surfaces for immunocapture of target bacterial species and subsequent separation of the target species from complex water samples (i.e. process water). Previously, support media for antibody-based sensors have included the surfaces of magnetic beads, microplates, and glass slides, and their applications include natural waters and sediments (Mazurek, 1996; Bard and Ward, 1997; Liu, et al, 2001; Favrin, et al, 2003; Furtado and Casper, 2000). In source water applications, biomolecule detection often requires both isolation and concentration of the target biomolecule to mitigate interference in complex water samples and cross-reactivity from competing analytes. Therefore, separations processes are needed with adjustable affinity properties specific to the analyte of interest.

**Note:** Initially, this work was to involve hydrogels as a support medium for biosensors as reflected in the project title. However, preliminary data indicated that this approach would not be viable since it was difficult to distribute biorecognition molecules evenly throughout the hydrogel matrix. In addition, the hydrogel pores became readily blocked in samples of moderate complexity. Therefore, the project was modified and combined with an ongoing project focused on development of a **novel** fouling-resistant membrane by attaching a polymer brush (hydroxypropyl cellulose) on the surface.

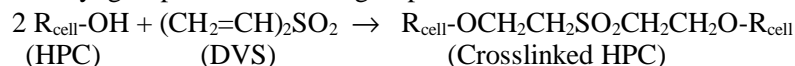
**RESEARCH OBJECTIVES.** *The goal of this proof-of-concept study was the synthesis, characterization, and performance evaluation of a novel membrane-based sensor for the specific detection of biomolecules.* The membranes were modified with a polymer brush (hydroxypropyl cellulose) on the surface, which acted as the support medium for bacterial sensing. To our knowledge, this is the first application of conjugated polymers attached to membranes for bacterial sensing. This technology can easily be translated to small membrane coupons or hand-held membrane based sensing devices. There were three main goals of this work: (i) develop chemistries to bind HPC to the membrane surface, (ii) demonstrate covalent binding of a model biorecognition molecule (antibody) to the brushes on membrane surface and (iii) demonstrate that the antibody-HPC modified membrane can immobilize the target organism.

## EXPERIMENTAL

This work focused on detailed synthesis and characterization of individual components for a model membrane system (cellulose acetate).

### *Objective 1: Develop Methods to Modify the Membrane Surface with Polymer Brushes*

Free standing crosslinking of HPC with DVS can be formed. The results for free standing gels was compared to those for the modified membranes. The reaction with either CA or HPC occurs by addition of vinyl group of DVS to OH group of cellulose as shown in the following reaction (Kabra, 1993):



When used to crosslink HPC and other cellulose ethers in isotropic aqueous solutions, DVS forms gels at pH 12 in less than an hour. These results suggested that it is possible to crosslink HPC with DVS fast enough by keeping the pH of the mixture high. This chemistry was modified for modified to allow for modification of the cellulose acetate membranes as described below.

The membranes were modified using a method sequential coating method. The membranes were coated with a (0.5 – 1.5) weight-percent DVS solution, washed thoroughly with ethanol and coated with a 7-10 weight percent HPC (MW=100,000) solution. While a high MW HPC chain was used to ensure good extension from the membrane surface at low temperatures, the length of the HPC can also be varied to modify surface properties. The DVS reaction time was varied from 30 minutes to 6 hours to modify the surface density. The coating was allowed to dry for 48 hours and after drying, the membranes were kept overnight in DI before running.

### *Objective 2: Membrane Characterization*

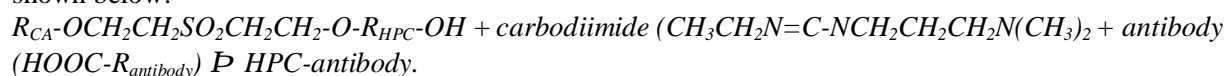
- ATR-FTIR was used to probe the evolution in chemical structure of the covalently bound polymer brush and CA surface that constitutes the surface of the membrane. FTIR uses measurements of vibrational spectra to identify the chemical structure of materials. The ATR attachment allowed measurement on the top surface layer of membrane. Measurement was performed using a Digilab UMA 600 FT-IT microscope with a Pike HATR adapter and an Excalibur FTS 400 spectrometer.
- AFM provides an easy and fast method to observe the surface structure of a wide range of materials. AFM allows acquiring 3D topographic data with a high vertical resolution. Accurate and quantitative data about surface morphology are provided over a wide range of magnifications and can be used in several quantitative analyses approaches such as section, bearing and roughness analysis. AFM measurement was performed using a Nanoscope IIIa Scanning Probe Microscopy in the Department of Chemical Engineering at the University of Toledo.

### *Objective 3: Sensor Development and Testing*

Bacterial culture *Mycobacterium parafortuitum* (#19688) was ordered from American Type Culture Collection (ATCC). The culture was grown at 37°C on Lowenstein-Jenson solid media (BD 220908, BD) and in MiddleBrook 7H9 broth (#R061346, Remel Inc, KS).

A model biorecognition molecule (i.e. antibody) was selected for attachment to the membrane and subsequent immobilization of mycobacteria for detection. The primary polyclonal antibody (rabbit anti-mycobacterium IgG #6398-0006, Biogenesis, NH) was selected for this work (Yi et al., 1998). Fragments of goat anti-rabbit IgG (H+L) antibodies with a fluorescent tag (Alexa Fluor<sup>®</sup> 594) were used as secondary antibody for verification of primary Ab attachment to the modified membrane surface. Secondary antibodies (Ab) were obtained from Invitrogen<sup>™</sup> (#A11072, Invitrogen Corporation, IL).

A carbodiimide (CDI) was chosen to attach the antibody the surface bound HP. The reaction chemistry is shown below:



Specifically, the CDI is a zero-length linker that facilitates the reaction between hydroxyl groups (i.e. the brush) and carboxyl groups (i.e. the antibody). For this reaction, the CDI was dissolved in buffer solution, applied to the membrane and placed in the antibody (Ab) solution (concentration?). FTIR with ATR was used to monitor the membrane following each reaction step.

The antibody-HPC modified membrane was tested for its ability to detect *mycobacteria*. The protocol for determining the recovery of target microorganisms using an immunoassay was modified from Yi et al. (1998). The membranes (25mm diameter) were manipulated in 6-well cell culture plates. 1mL of concentrated bacteria ( $7.7 \times 10^5/\text{mL}$ ) in laboratory grade water was added to the surface of the membrane and incubated for up to 90min covered on a shaker table. After incubation, the antibody-HPC modified membrane was rinsed 3X with and resuspended in 1mL of laboratory grade water. 2uL of a DNA intercalating stain (Picogreen<sup>®</sup>, Invitrogen, Chicago, IL) was added and incubated for 5min to detect bound bacteria. In replicate samples, fluorophore labeled secondary antibody (Leinco, USA) was added at varying dilutions (1:10 to 1:200) and incubated for 30min at room temperature to verify the presence of the antibody on the membrane surface. Samples were processed on a fluorescent microscope. Control samples for this experiment included: unmodified membrane, membrane modified with HPC only, antibody-HPC modified membrane. Non-specific binding of mycobacteria to the unmodified membrane and the membrane modified with HPC only was negligible.

## RESULTS AND DISCUSSION

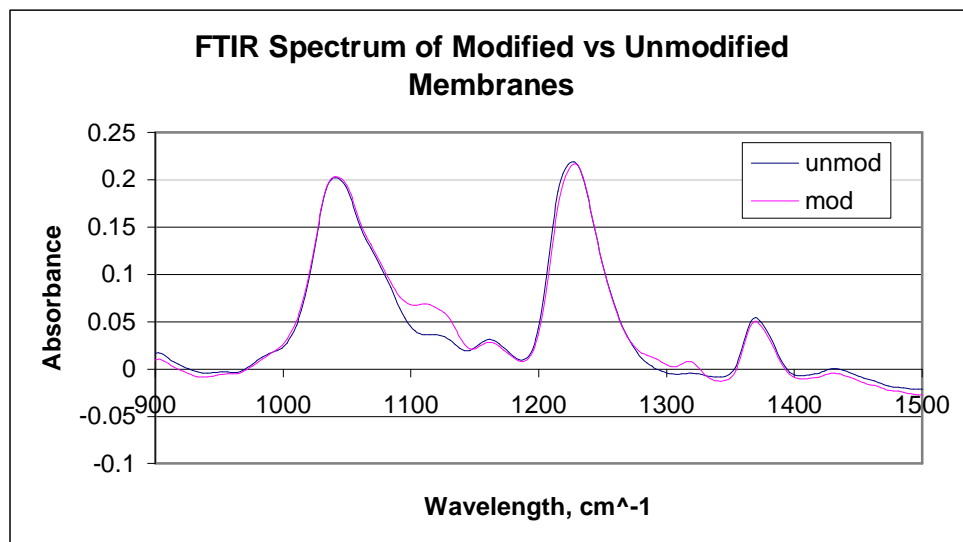
The project goal was to determine the viability of the *novel* idea of combining a brush on membrane for fouling resistance with a biosensor component to detect potential biofouling species.

### *Formation of Brushes on Membrane Surface*

The membrane used for the preliminary work was a hydrophilic cellulose acetate (CA) ultrafiltration membrane with a molecular weight cutoff (MWCO) of 20,000 Daltons. The membrane surface was modified with the polymer brush, hydroxypropyl cellulose (HPC) via a divinylsulfone spacer (DVS). As an initial step, crosslinked gels of DVS and HPC were produced using standard chemistry reported in literature (Kabra 1993). While the DVS acts as a linker molecule between the membrane surface and the

HPC brushes in the system of interest, it is used initially as a crosslinker to form bulk free standing gels of HPC. The next step was to functionalize the CA membrane with HPC via the DVS spacer and characterize the HPC-modified membrane using FTIR. Since the

structure of HPC and the CA are very similar, modification was verified using FTIR analysis of the peak for the sulfonic bond of DVS. The adjacent FTIR spectra shows the onset of peaks for  $\text{SO}_2$  bond in two locations at  $1130$  and  $1315 \text{ cm}^{-1}$  following exposure of CA membrane to DVS in NaOH solution for one hour followed by exposure to HPC.

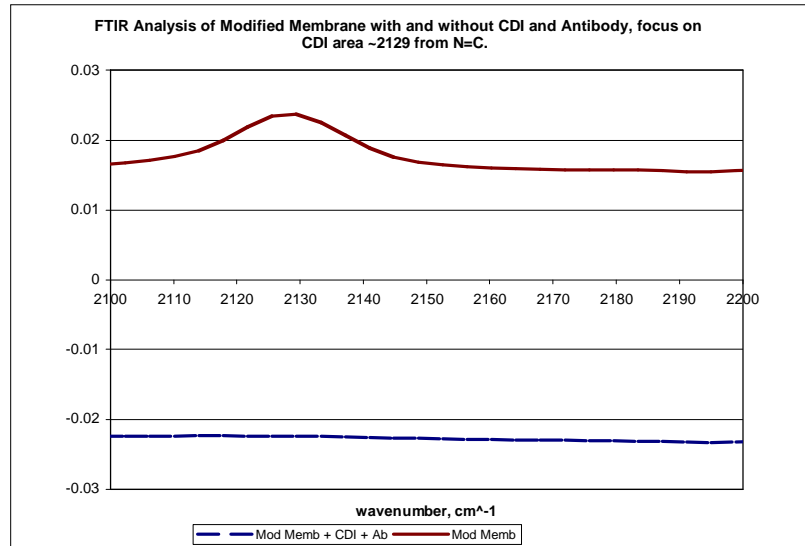


#### *Attachment of Model Biorecognition Molecule*

A model biorecognition molecule (i.e. antibody) was attached to the membrane and to verify the ability of the membrane-based sensor to detect bacteria. While a number of chemistries are available to attach the antibody the surface bound HPC, a carbodiimide (CDI) was chosen. Fourier transform infrared spectroscopy was used to monitor the membrane following each reaction step.

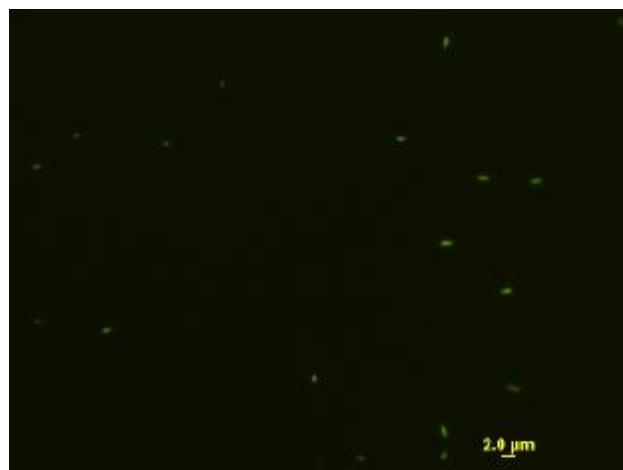
The only peak that was affected was at  $2129\text{ cm}^{-1}$ . Since the CDI is acting as a zero-length linker, we hypothesize that the appearance of the peak at  $2129\text{ cm}^{-1}$  is due to the brush binding to the antibody.

In addition, fluorescently-labeled secondary antibody was added to the antibody-HPC modified membrane and an unmodified membrane for comparison. It was determined that primary antibodies were immobilized on the antibody-HPC modified membrane and were available for binding since approximately  $4 \times 10^5$  fluorescently-labeled secondary antibodies remained on the membrane.



#### *Mycobacteria Detection with Antibody-HPC Modified Membrane*

The antibody-HPC modified membrane was tested for its ability to bind *mycobacteria*. After multiple experiments with a range of initial mycobacteria concentrations ( $1 \times 10^5$  to  $1 \times 10^7$ /mL) approximately 10% were recovered on the antibody-HPC modified membrane surface.



***mycobacteria* were captured on the surface of antibody-HPC modified membrane (1000X)**

### **SIGNIFICANCE AND IMPACTS OF RESEARCH ACTIVITIES**

The project produced a fouling-resistant membrane by attaching a polymer brush on the surface. Biorecognition molecules targeting selected bacteria were covalently bounded to the end of polymer brushes for in situ detection. Typically, the biological recognition component consists of enzymes, receptors, nucleic acids, or antibodies specific to biological markers.

Our proposed membrane modification/sensing technique developed stronger membranes capable of withstanding harsh raw water quality conditions without losing their reliability in producing a high quality safe product. Although the research outlined in this proposal addresses detection of biological contaminants in water treatment systems, the sensor developed from this work can be adapted to address a range of national and international environmental concerns.

### **ACKNOWLEDGEMENTS**

This materials portion of this project was funded by NSF CBET SGER 0610624.

# The Scour and Deposition River and Estuarine Bridges

## Basic Information

<b>Title:</b>	The Scour and Deposition River and Estuarine Bridges
<b>Project Number:</b>	2006OH39B
<b>Start Date:</b>	3/1/2006
<b>End Date:</b>	2/28/2008
<b>Funding Source:</b>	104B
<b>Congressional District:</b>	15th
<b>Research Category:</b>	Engineering
<b>Focus Category:</b>	Geomorphological Processes, Sediments, None
<b>Descriptors:</b>	
<b>Principal Investigators:</b>	Diane L Foster, Thomas C Lippmann

## **Publication**

1. Hatton, K. A. and Foster, D. L., 2006, Vertical Pile Scour Induced by Random Free Surface Gravity Waves, in 30th Int. Conf. Coastal Engin. ASCE.
2. Hatton, K. A., Foster, D. L., Traykovski, P. A., and Smith, H. D., 2007, Scour and Burial of Submerged Mines in Wave Conditions, IEEE Journal of Ocean Engineering.
3. Hatton, K. A. and Foster, D. L., 2007, Scour and Ripple Migration Offshore of a Vertically Mounted Pile Subjected to Irregular Waves, Journal of Hydraulic Engineering, ASCE, in review.
4. Hatton, K. A. 2006, Vertically Mounted Pile Scour Subjected to Irregular Waves, M.S. Thesis, The Ohio State University. Dept. of Civil and Environmental Engineering and Geodetic Science, The Ohio State University. Columbus, OH.

## **WRI Annual Report, June 22, 2007**

### **“The Scour and Deposition around River and Estuarine Bridges”**

Drs. Diane L. Foster and Thomas C. Lippmann  
Ohio State University

#### **Problem and Research Objectives**

This investigation is motivated by the amount of river, estuarine, and coastal infrastructure that is susceptible to extreme wave and flooding events. The high velocities and resulting shear stresses associated with high flow velocities are capable of scouring or depositing large quantities of sediment around hydraulic structures. Preventing the failure of these structures and sedimentation in inlets alone costs federal and state agencies billions of dollars annually. In addition to being costly, the manual monitoring of bridge scour - as mandated by the Federal Highway Administration - can be inefficient in states such as Ohio where the flood events that initiate the scour process occur sporadically. According to the National Scour Evaluation Database, there are 23326 bridges over waterways in the state of Ohio, of which 5273 are considered scour susceptible and 191 are considered 'scour critical'.

Previous methods for identifying bridge scour have relied on the manual (diver-based) sampling of local water depths that are generally limited to periods of low water flow. As the dynamic scour and deposition of sediments around structures is highest during periods of high flow, traditional sampling methods have limited our ability to predict quantitatively scour or deposition levels and to evaluate sediment transport models.

Related to problems generated by sediment scour are issues of sediment deposition in navigational channels. On the Maumee River, OH, alone, the Army Corp of Engineers spends millions of dollars annually to dredge an average of 850,000 cubic yards of sediment. With the elimination of open lake disposal of dredged sediments, an inter-agency collaboration of government and private citizens has been formed to identify possible methods for reducing the amount of deposition by reducing the soil erosion along river bank's. Clearly, an increase in our understanding of how sediment is scoured or deposited around structures will improve our ability to utilize available resources in

The overall objective of this research is to increase our ability to predict how variations in flow conditions will affect the scour and/or deposition of sediment around estuarine and river bridges. Specific goals for this project are:

1. Observe the flow field and morphologic variability induced by high water flows at bridge ODOT ID-BUT-128-0855 located on the Great Miami River in Hamilton, OH, using a suite of acoustic, video, and bathymetric survey instrumentation.

2. Simulate the three-dimensional flow and sediment transport surrounding both cylindrical and ellipsoidal bridge piers using a highly evolved CFD numerical model (Flow-3D, Flow Science, Inc.). The model simulations will be forced by and evaluated with laboratory observations obtained in a large wave flume in the summer of 2005, and with the field observations obtained in the first objective of this proposal.
3. Examine the effect variations in river stage will have on bridge scour. Particular attention will be paid to locations where the near field, but larger scale, river geomorphology results in complex three-dimensional velocities near the bridge piles.

## Methodology

Modeling of the scour and depositional process is being performed with the computational fluid dynamics model FLOW-3D (Flow Science, Santa Fe, NM). FLOW-3D is a three-dimensional, non-hydrostatic computational fluid dynamics model that employs the FAVOR method to resolve the flow around obstacles without mesh regeneration. The primary strength of FLOW-3D is its ability to accurately resolve three-dimensional flows in great detail, while tracking complex flow behavior at fluid-structure and fluid-sediment interfaces. The flow-sediment-structure modules allow for coupled flow-sediment equations to be incorporated.

First, the model is being used to simulate the flow and sediment scour surrounding a single vertical pile with an initially flat bed. Laboratory observations obtained at a collaborative full-scale laboratory experiment, CROSSTEX, are used to evaluate the model. The fluid forcing for the model is provided by the observed free stream flow under random wave conditions. The modeled flow field is evaluated with *insitu* observations of the two-dimensional flow field upstream of the vertical pile (obtained with a Particle Image Velocimetry, PIV, system; **Figure 1**). The modeled sediment transport is evaluated with observations of suspended sediment and seabed elevations obtained by a two-axis variable frequency sonar.

In CROSSTEX, the flow and scour surrounding a vertical pile was measured under forcing by random free surface gravity wave fields. The observations were obtained in the shoaling region in approximately 1.5 m water depth of a 104 m long, 3.7 m wide flume at the O.H. Hinsdale Wave Research Laboratory. The 6 cm pile was placed in an erodible sand bed with a median grain size diameter of 0.1 mm. A Particle Image Velocimetry (PIV) system consisting of a camera focused on a laser sheet was used to observe the two-dimensional (x-z) time dependent flow fields at 3 Hz. A two-axis variable frequency acoustic backscatter sensor observed the sediment suspension at 1 cm range bins over the x-z plane and the bed geometry over a 1 m range in the x-y plane. Figure 1 shows a schematic of the underwater instrument deployment. The field of view for the PIV system was a 23 cm x 23 cm plane offshore of the pile.

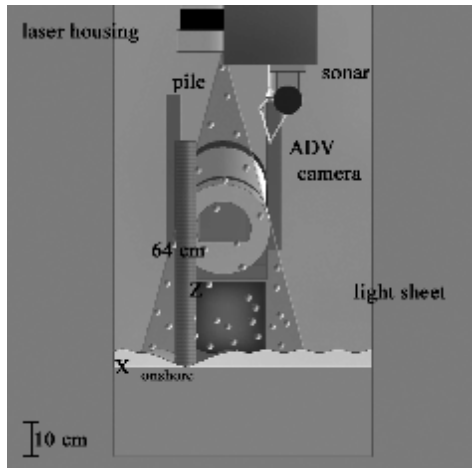


**Figure 1.** Snap shots of the  $x$ - $z$  velocity field and bed geometry upstream of a vertically oriented cylinder (indicated by the gray shaded region in each panel) at (left) the initiation of sediment motion and (right) the equilibrium profile. Both images are taken during the wave crests. Red vectors represent the highest velocities, blue the lowest. The dashed line represents the still bed profile on the unrectified image.

Secondly, the model is being used to simulate the morphologic evolution of the Great Miami River bed (in Hamilton, OH) in response to observed high flows. This situation is more complicated than the laboratory setting because of the large variability in the initial morphologic state and because of the large amount of flow disturbances generated by the detritus present on the riverbed. The initial scour simulations will follow the bed load transport calculations of Hatton *et al.* (2007). Regions of potential scour will be identified when the local bed stress exceeds the critical bed stress. Regions of potential deposition will be assumed when the Rouse number is of order 10.



**Figure 2.** The WaveRunner survey system is capable of measuring water depths from approximately 0.4 m to 15 m.

In this investigation, the model geometry is being initialized with observed river bathymetry obtained from an in-hand bathymetric survey system consisting of a Yamaha GP1200 WaveRunner equipped with differential GPS receiver, dual-transducer sonic altimeter, and custom navigation software (**Figure 2**). As part of previous research efforts,

the system has been utilized extensively in coastal marine and fresh water environments where waves and currents are present (and sometimes energetic). The system has accuracies of about  $\pm 5\text{-}7\text{ cm}$  in both the horizontal and vertical coordinates of the measured bathymetry.

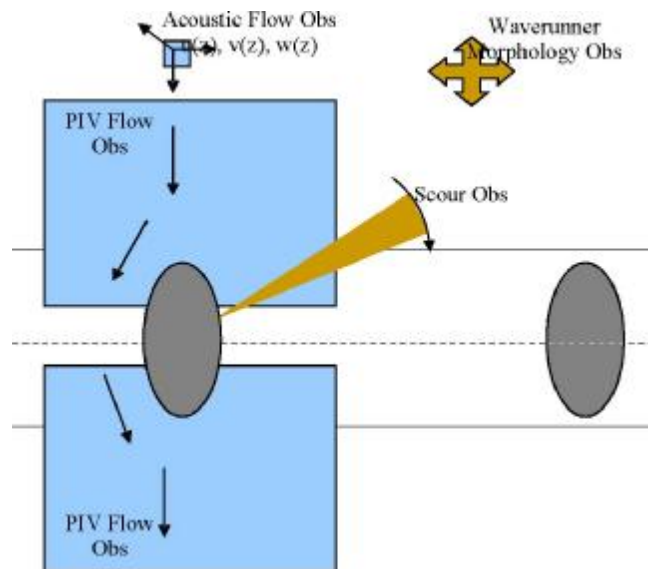


**Figure 3.** 2-D schematic of proposed deployment strategy at the Great Miami River bridge in Hamilton, OH. The hypothetical bridge piles are indicated by the gray-shaded ellipses. Blue highlighted areas represent regions where surface flows will be made with video-based PIV techniques. The yellow highlighted wedge represents a single slice of the IMAGENEX sonar used for local scour observations. Far-field bathymetric observations will be obtained with the WaveRunner survey system.

Field observations of surface flow and local scour have been obtained during a field deployment. A schematic of the experimental design is shown in **Figure 3**. Vertical profiles of velocity can be measured at a single upstream location with a Pulse-Coherent Acoustic Doppler Profiler (PC-ADP). The sensor can remotely sample three-components of velocity at  $5\text{ cm}$  range bins at a  $2\text{ Hz}$  sampling rate. The observations can be used to specify the upstream boundary condition and be compared with observations of the surface flow. Measurements of the surface flow in and around the pier piling will be obtained from analysis of video data that utilizes PIV techniques. The recently developed PIV system uses visible particles on the water surface (such as from sediment patches, bubble clouds, or other passively floating detritus) to identify displacements between individual frames of the video imagery. Correlation and filtering techniques have been developed that allow mean and oscillatory flow to be measured with high accuracy, on the order of 10% of the measured velocity field.

For this project, cameras will be deployed on both the upstream and downstream sides of the bridge (**Figure 3**). The labor intensive nature of the PIV system will limit surface flow analyses to the initial model evaluation and to several high-flow events. The near-field scour and sediment suspension was measured with a rotating two-axis IMAGENEX profiling sonar attached to the bridge pier (**Figure 4**). The sonar will resolve the two-dimensional centimeter-scale bathymetric variations over a 5-20 m radius.



**Figure 4.** Snapshot of an IMAGENEX deployment at the proposed Hamilton site (ODOT ID-BUT-128-0855). Figure courtesy of Dave Straub (USGS).

The instrumentation will be deployed during one low flow event and several high flow events. Observations will be used to evaluate model performance as well as identify any flow patterns related to structure scour and deposition. Model simulations will also be qualitatively compared with observations from the National Bridge Scour Database (USGS). Ongoing model-data comparisons will improve model strengths and set limitations on present capabilities. Following successful model-data comparisons, the model can be used to predict the scour and deposition around bridge piers for extreme storm events with a variety of return periods that may include, for example, 20, 50, or 100 year events.

### **Principal Findings**

Hatton and Foster (2007) observed the bed evolution offshore of a vertical pile subjected to five different forcing conditions. Bed evolution was resolved over a 23 cm by 23 cm window offshore of a 6 cm diameter vertical pile with our submersible PIV system. The duration of wave generation was long enough for each data set to reach equilibrium scour depths. In each of the five sets of observations, ripples migrated onshore towards the scour depression to a distance of one-half of a ripple wavelength from the scour depression, remaining roughly static until a series of larger waves causes the ripple to merge with the

scour hole ( $\theta_{2.5} > 0.45$ ) or plane off the bed ( $\theta_{2.5} > 0.8$ ). **Figure 5** shows an example of ripple-scour mergers. Following the initial growth of the ripple field ( $t/T = 75$ ), the offshore-most ripple (at  $x=15$  cm) migrates onshore towards the growing scour pit at a rate of 0.6 cm/min until the ripple crest is within one-half of a wavelength from the edge of the scour pit ( $t/T = 120$ ). At this point, the ripple stops migrating and the scour hole stops growing until a series of larger waves causes the ripple to merge with the scour ripple ( $t/T=200$ ). These mergers occur at grain roughness Shields parameters ( $\theta_{2.5}$ ) of more than 0.45 and cause fluctuations in the scour hole width. Bed planing events ( $\theta_{2.5} > 0.8$ ) also lead to fluctuations in the scour width, but are accompanied by an increase in scour depth. These limited observations are the first full-scale observations of wave-induced ripple migration into a scour depression. The observations provide further support for the dependence of bedform evolution on the vortex dynamics and provide a valuable basis for the further study of bedform evolution in competitive environments.

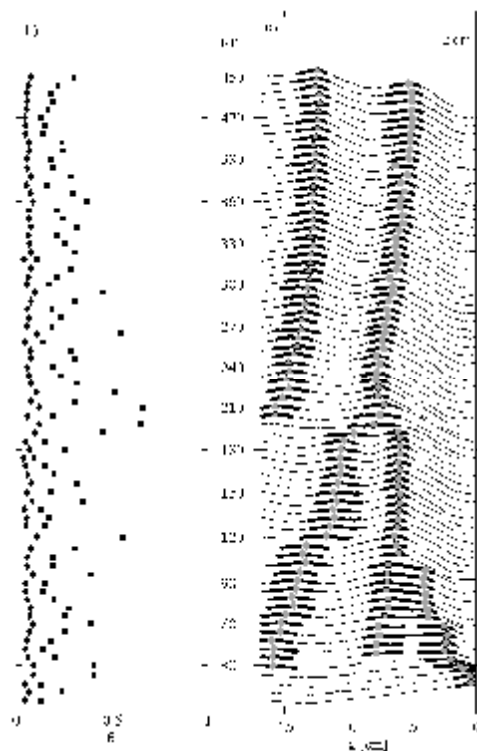


**Figure 5.** Bed profiles and forcing for irregular waves ( $H_{mo} = 30$  cm and  $T = 4$  s). The Shields parameter,  $\theta$ , ( $\mathbf{u}$ ) and grain roughness Shields parameter,  $\theta_{2.5}$ , ( $\mathbf{n}$ ) for each consecutive, 24 s window. (c) Vertically offset timestacks of 24s averaged 2-D bed profiles (solid black lines). The scour ripple local maximum and first, second and third offshore local maxima are represented with  $\Phi$ ,  $\mathbf{n}$ ,  $\mathbf{u}$ , and  $\mathbf{}$ , respectively. The solid black dots show the locations where the elevation is within 10 pixels of an individual local maximum.

We have simulated the response of the fine scale flow field and local morphology around submerged objects in both two- and three-dimensional environments. In the two-dimensional mode, the flow around fixed, scoured bed profiles is simulated and compared favorably with laboratory observations. These results show that the CFD model (FLOW-3D) well captures the complexities of flow very near the bed and around objects placed close to or on the seabed. **Figure 6** shows a simulation of wave-induced scour surrounding a horizontal pipeline. The simulations show that the vorticity structure evolves with the scouring bed (Smith and Foster, 2007). In the three-dimensional mode, the flow and scour of sediment beneath a cylindrical object lying on an initially flat bed is

simulated and compared with laboratory observations that show excellent agreement in mean flow characteristics (Hatton et al, 2007). This work demonstrates the capabilities of the numerical model to accurately resolve fine scale flows near obstacles (vertically or horizontally oriented) impinging on bottom topography with arbitrary form and with unconsolidated sedimentary material.

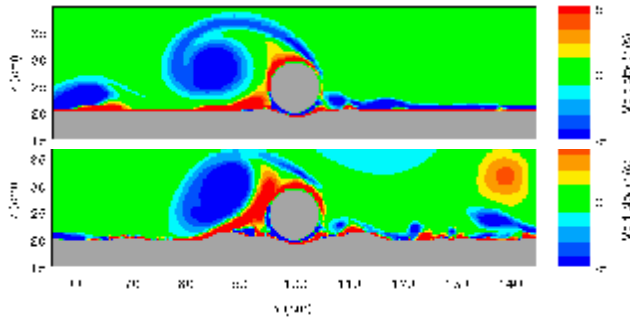


**Figure 6.** The vorticity surrounding a two-dimensional pipeline resting on a scouring seabed during the initial (top) and later (bottom) phase of scour hole development in wave environments. Both images are taken at the same flow phase as the flow is reversing from left to right.

Numerical model results for combined wave-current flow about a vertical pile are in qualitative agreement with prototype laboratory observations, suggesting that the model is well reproducing the essential flow characteristics and sediment transport. In contrast, *in situ* acoustic observations of river topography at a bridge pier located on the Great Miami River (near Hamilton, OH), where wave motions are minimal and river flow is approximately unidirectional and steady, show a distinct region of deposition of sedimentary material just upstream of one of the pier pilings. This qualitative result suggests that deposition and scour around bridge piers in natural rivers can be significantly altered by the presence of large debris.

River and bank surveys of the Great Miami River at Hamilton, OH, were completed on August 9, 2006. The river survey was conducted with the Coastal Bathymetry Survey System (CBASS, described earlier), and the bank survey was conducted by walking with a backpack-mounted differential GPS receiver and antenna. The survey spans about 1.2 km along the river, and was done over 2.5 hours with about 60 cross-river transects spaced every 20 m. The river edge was surveyed by walking along and down the bank where accessible.

GPS-based bathymetry surveying is made difficult at the Hamilton site due to line of sight blockage of the GPS satellite constellation under and near the bridge. In past surveys this has resulted in sparse bathymetry data near the bridge because of positional uncertainties. Sonar data are collected for these areas, however, the lack of accurate positional data rendered the depths useless for producing accurate river topography.

To improve the survey in the areas near and under the bridge, a navigational method known as dead-reckoning was adapted from techniques developed over 500 hundred years ago by sailors to navigate open seas. Dead-reckoning is still used today, but now in combination with other navigational aids such as GPS and inertial systems. This method

requires an initial known position and an assumed trajectory that does not vary in speed and direction. A simple form of dead-reckoning utilizes a measured velocity vector, then integrates the spatial positional components over a finite time scale to find the corresponding location associated with a particular time; in our case the time when the depth measurements were made.

In our methods, the initial and final positions of particular along river transects are known from the fixed GPS positions at times before the signal drop out under the bridge and the on the other (lea) side of the bridge when the signal is re-acquired. Velocity is maintained (and assumed) constant by the survey vehicle operator until a fixed position is established again. The vehicle is kept on a constant heading using visual landmarks by the operator to minimize spatial deviations from the assumed trajectory. An example of survey tracks used in our techniques is shown in **Figure 7**.

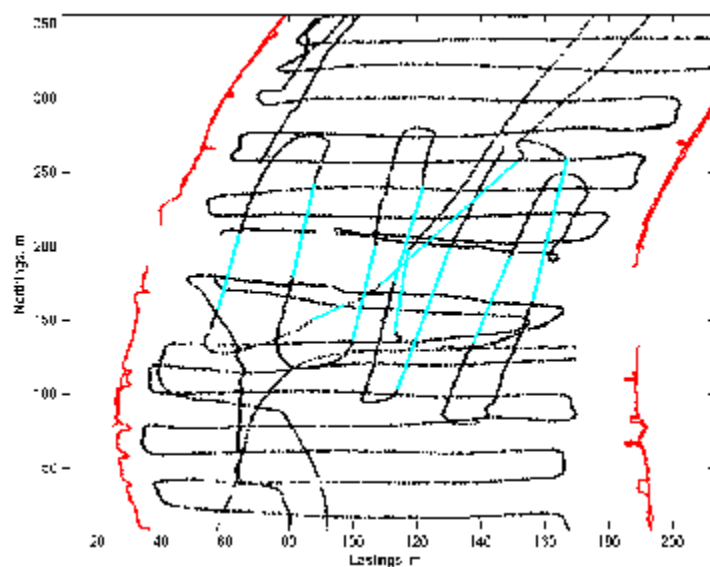


**Figure 7.** Close up plot of the survey tracks. Red tracks indicate walking survey, the black tracks indicate CBASS survey, and the cyan tracks indicate interpolated positions based on the dead-reckoning technique.

The distance and heading between the last two known points,  $(x_0, y_0)$  and  $(x_1, y_1)$  respectively, can be easily calculated. The times of these two points are taken from the GPS record, and the times along this line are calculated based on the desired number of points and sampling frequency. The sonar record is then interpolated to these times and depths are extracted for the specified times. **Figure 8** shows a schematic of the simple dead-reckoning geometry used to interpolate intermediate points.

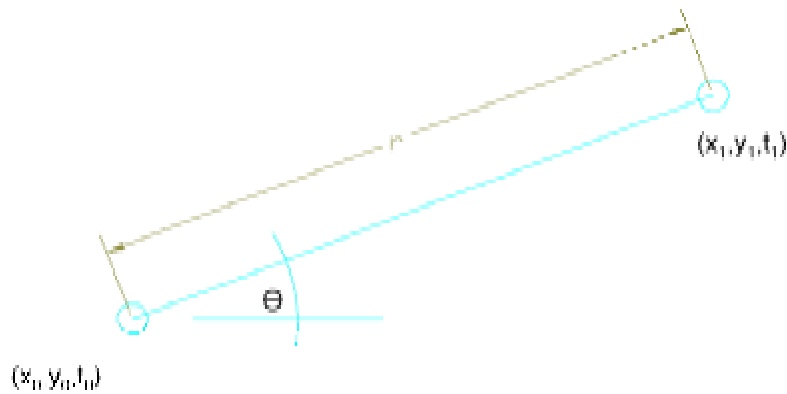


**Figure 8.** Illustration showing two known points along with the heading and distance between them.

This pseudo dead reckoning technique proved to work well. **Figure 9** shows the completed time series of water depths measured by the sonar from both the fixed GPS positional data (black dots) and the interpolated data (red dots) using the dead-reckoning approach. **Figure 10** then shows the completed bathymetric survey of the Great Miami River at Hamilton including the survey data obtained beneath the bridge with positions determined from the dead-reckoning approach. This technique, with our current equipment, is limited to areas that the water surface can be assumed flat because there is no way to determine fluctuations in water surface elevation (*i.e.*, waves). The incorporation of an inertial system may allow this technique to be effective in the presence of waves.

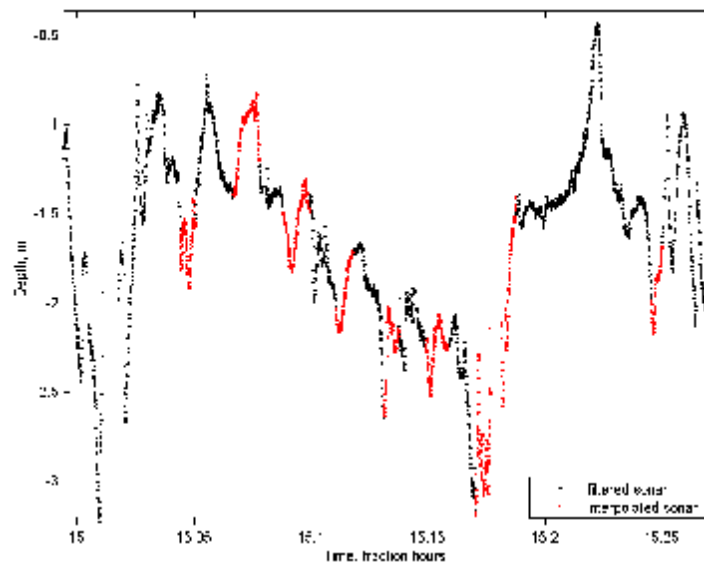


**Figure 9.** Sonar data from CBASS. The black points are the data from the known  $x/y$  positions and the red points are the data extracted from the sonar record based on the interpolated spatial and temporal points.

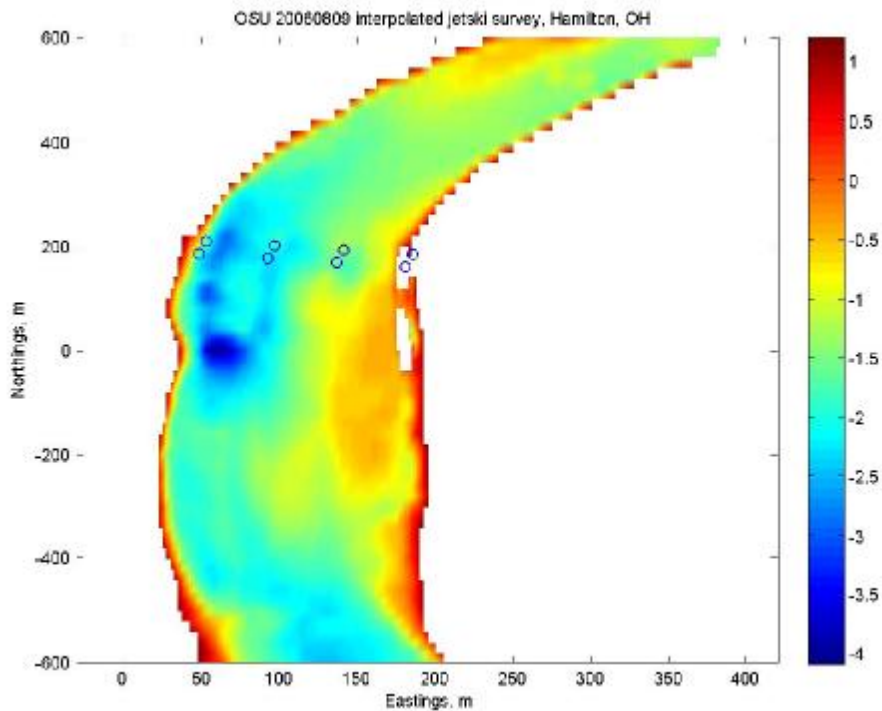


**Figure 10.** Interpolated river bathymetry including sonar data under the bridge from dead reckoning technique.

Finally, mean surface velocity vectors of the river flow just upstream of the bridge at Hamilton have been initially estimated using Particle Image Velocimetry (PIV) techniques developed for oceanic applications. Continued development of the techniques for river applications is underway, and will be verified from manual tracking of obvious surface features in the flow (the manual methods being required owing to lack of *in situ* observations of the flows). These observations will be used to initialize the model and coupled with observations of the river bathymetry obtained with the CBASS survey system.

### Significance

The coupling of detailed flow and bed elevation observations with a numerical fluid-sediment model will improve our understanding of the scour process. We also anticipate that engineers and river managers will use improved scour predictions to improve structural design, streamline mitigation procedures, and reduce response times to predicted high flow events by focusing resources to high scour regions. The results may also be used to select locations for future sampling sites, and to identify those sites where scour is expected to be problematic for future structural integrity. Our field and modeling methods represent new ways to monitor and evaluate bridge scour, and together these

model-data results will highlight potential areas of concern.

## **Information Transfer Program**

The Ohio Water Resources Center (WRC), at Ohio State University, conducted a number of activities to transfer water related information to a wide range of state, federal, county, and municipal agencies, to the private sector, academic community, students, and to private citizens throughout Ohio. Specific activities included,

- preparation of information for the web site of the Ohio Water Resources Center and maintenance of the web site
- administration of a Special Water and Wastewater Treatment Grants Competition funded through the Ohio Water Development Authority
- administration of the 104(B) In-State Competition and the 104(G) National Competitive Grants Program
- encouraged investigators of projects funded through the Ohio WRC to develop publications in peer-reviewed journals and other outlets
- continued administrative support for the Water Management Association of Ohio (WMAO) and associated WMAO meetings, conferences, and division activities
- support for Ohio Water Education Program, especially Project WET (Water Education for Teachers)
- participation of both directors in the Future Engineers Summer Camp (FESC) which focuses on introducing 8th grade girls to careers in various areas of engineering, including water resources and environmental engineering
- responding to questions from the public regarding water resources issues in the state of Ohio

## Student Support

Student Support					
Category	Section 104 Base Grant	Section 104 NCGP Award	NIWR-USGS Internship	Supplemental Awards	Total
Undergraduate	7	0	0	0	7
Masters	3	0	0	0	3
Ph.D.	3	0	0	0	3
Post-Doc.	0	0	0	0	0
<b>Total</b>	13	0	0	0	13

## Notable Awards and Achievements

Project "The scour and Deposition around River and Estuarine Bridge" (2006OH39B): Kim Hatton (Seidelmann) who is a Master student supported by this project received National Science Foundation Graduate Fellowship.

## Publications from Prior Projects

- 2005OH16B ("Transport and Fate of Iron Nanoparticles in Groundwater") - Dissertations - Regan Welch. 2007. Reduction of 2,4,6-trinitrotoluene with nanoscale zero-valent iron. M.S. Thesis. Department of Civil Engineering, Ohio University.
- 2005OH16B ("Transport and Fate of Iron Nanoparticles in Groundwater") - Conference Proceedings - Riefler, R. Guy, and Reagan Welch. 2007. Reduction Capacity of Iron Nanoparticles Treating TNT. in Association of Environmental Engineering and Science Professors Interactions at the Interface Conference. Blacksburg, VA.
- 2005OH27B ("Technology Enhanced Participation for Watershed Planning") - Articles in Refereed Scientific Journals - Higgs, Gary. 2006. Integrating multi-criteria techniques with geographical information systems in waste facility location to enhance public participation. Waste Management & Research, Vol. 24, No. 2, 105-117
- 2005OH26B ("USE OF PERSULFATE AND PEROXYMONOSULFATE OXIDANTS FOR THE DESTRUCTION OF GROUNDWATER CONTAMINANTS") - Dissertations - Choi, Hyeok. 2007, Novel Preparation of Nanostructured Titanium Dioxide Photocatalytic Particles, Films, Membranes, and Devices for Environmental Applications, Ph.D. Dissertation, Dept. of Environmental Engineering, University of Cincinnati.
- 2005OH26B ("USE OF PERSULFATE AND PEROXYMONOSULFATE OXIDANTS FOR THE DESTRUCTION OF GROUNDWATER CONTAMINANTS") - Articles in Refereed Scientific Journals - Qiuqing Yang, Hyeok Choi, Yongjun Chen, Dionysios D. Dionysiou, 2007, Heterogeneous activation of peroxymonosulfate by immobilized cobalt: The effects of support, cobalt precursor and UV irradiation. Submitted to Applied Catalysis B: Environmental.
- 2005OH26B ("USE OF PERSULFATE AND PEROXYMONOSULFATE OXIDANTS FOR THE

- DESTRUCTION OF GROUNDWATER CONTAMINANTS") - Conference Proceedings - Dionysios D. Dionysiou, George P. Anipsitakis, Aditya Rastogi, Qiuqing Yang, and Souhail Al-Abed, 2007, Sulfate Radical-Based Advanced Oxidation Processes. Invited Presentation at the ACS and AIChE Symposium on Applied Chemistry and Engineering, Division of Industrial and Engineering Chemistry Research, in 233rd American Chemical Society National Meeting (ACS), Chicago, Illinois. paper 35.
7. 2005OH26B ("USE OF PERSULFATE AND PEROXYMONOSULFATE OXIDANTS FOR THE DESTRUCTION OF GROUNDWATER CONTAMINANTS") - Conference Proceedings - Aditya Rastogi, Souhail R. Al-Abed, Dionysios D. Dionysiou, 2007, Destruction of PCBs using sulfate radical-based advanced oxidation processes, Oral Presentation at the Symposium on Sustainability in Water Supply: Advances in Oxidation Processes for Water Treatment, Division of Sustainability of Energy, Food and Water, in 233rd American Chemical Society National Meeting (ACS), Chicago, Illinois. paper 151.
  8. 2005OH26B ("USE OF PERSULFATE AND PEROXYMONOSULFATE OXIDANTS FOR THE DESTRUCTION OF GROUNDWATER CONTAMINANTS") - Conference Proceedings - Aditya Rastogi, Souhail R. Al-Abed, Dionysios D. Dionysiou, 2007, Development of Sulfate Radical-Based Chemical Oxidation Processes for Groundwater Remediation. Podium Presentation, in 80th Annual WEFTEC, San Diego, California.
  9. 2005OH21B ("Manipulating residence time in agricultural headwater streams: impacts on nitrogen removal and aquatic communities") - Dissertations - Herrman. K.S. 2007, Factors affecting nitrogen removal in headwater streams located in a fragmented agricultural landscape. PhD Dissertation, Ohio State University.
  10. 2005OH21B ("Manipulating residence time in agricultural headwater streams: impacts on nitrogen removal and aquatic communities") - Articles in Refereed Scientific Journals - Herrman, K., Bouchard, V., Moore, R. 2007, Factors that affect denitrification in agricultural headwater streams in Northeast Ohio, USA. *Hydrobiologia*, In revision.